



## Research article

# Single-cell RNA sequencing reveals heterogeneity of ALI model and epithelial cell alterations after exposure to electronic cigarette aerosol

Meng-yun Cai <sup>a,1</sup>, Xiaofan Mao <sup>a,1</sup>, Beiyong Zhang <sup>a,1</sup>, Chung-Yin Yip <sup>b,1</sup>, Ke-wu Pan <sup>b</sup>, Ya Niu <sup>b</sup>, Stephen Kwok-Wing Tsui <sup>b</sup>, Joaquim Si-Long Vong <sup>b</sup>, Judith Choi-Wo Mak <sup>c</sup>, Wei Luo <sup>a,\*\*</sup>, Wing-Hung Ko <sup>b,\*</sup>

<sup>a</sup> Institute of Translational Medicine, The First People's Hospital of Foshan, Guangdong, PR China

<sup>b</sup> School of Biomedical Sciences, The Chinese University of Hong Kong, Shatin, N.T., Hong Kong

<sup>c</sup> Department of Pharmacology & Pharmacy, The University of Hong Kong, Hong Kong

## ARTICLE INFO

## Keywords:

Bronchial epithelium  
e-cigarette  
Single-cell RNA sequencing  
Nicotine  
Flavoring  
Epithelial heterogeneity  
SARS-CoV-2

## ABSTRACT

Electronic cigarettes (e-cigarettes) have been advertised as a healthier alternative to traditional cigarettes; however, their exact effects on the bronchial epithelium are poorly understood. Air-liquid interface culture human bronchial epithelium (ALI-HBE) contains various cell types, including basal cell, ciliated cell and secretory cell, providing an *in vitro* model that simulates the biological characteristics of normal bronchial epithelium. Multiplex single-cell RNA sequencing of ALI-HBE was used to reveal previously unrecognized transcriptional heterogeneity within the human bronchial epithelium and cell type-specific responses to acute exposure to e-cigarette aerosol (e-aerosol) containing distinct components (nicotine and/or flavoring). The findings of our study show that nicotine-containing e-aerosol affected gene expression related to transformed basal cells into secretory cells after acute exposure; inhibition of secretory cell function by down-regulating genes related to epithelial cell differentiation, calcium ion binding, extracellular exosomes, and secreted proteins; and enhanced interaction between secretory cells and other cells. On the other hand, flavoring may alter the growth pattern of epithelial cells and make basal cells more susceptible to SARS-CoV infection. Besides, the data also indicate factors that may promote SARS-CoV-2 infection and suggest therapeutic targets for restoring normal bronchial epithelium function after e-cigarette use. In summary, the current study offered fresh perspectives on alterations in the cellular landscape and cell type-specific responses in human bronchial epithelium that are brought about by e-cigarette use.

**Abbreviations:** ALI-HBE, Air-Liquid Interface cultured Human Bronchial Epithelium; CBC, Ciliated Basal Cell; CSC, Ciliated Secretory Cell; BSC, Basal-like Secretory Cell; TSC, Terminal Secretory Cell; ISC, Intermediate Secretory Cell; GO, Gene Ontology; SBC, Secretory-like Basal Cell; IBC, Intermediate Basal Cell; PBC, Progenitor-like Basal Cell.

\* Corresponding author.

\*\* Corresponding author.

E-mail address: [whko@cuhk.edu.hk](mailto:whko@cuhk.edu.hk) (W.-H. Ko).

<sup>1</sup> Meng-yun Cai, Xiaofan Mao, Beiyong Zhang and Chung-yin Yip contributed equally to this work.

<https://doi.org/10.1016/j.heliyon.2024.e38552>

Received 23 April 2024; Received in revised form 18 July 2024; Accepted 25 September 2024

Available online 26 September 2024

2405-8440/© 2024 The Authors. Published by Elsevier Ltd. This is an open access article under the CC BY-NC license (<http://creativecommons.org/licenses/by-nc/4.0/>).

## 1. Introduction

Electronic cigarettes (e-cigarettes) are portable electronic devices comprising a battery, heater, and refillable cartridge containing an e-liquid, which usually consists of a solvent (propylene glycol or vegetable glycerol), nicotine, and flavorings [1,2]. Over the past decade, e-cigarettes have been advertised as a healthier alternative to traditional cigarettes and rapidly gained popularity worldwide, particularly among young people [3,4]. The negative effects of e-cigarette aerosol (e-aerosol) on human health were not taken seriously until an outbreak of e-cigarette-associated lung injury was documented in 2019 [5]. Soon after, during the outbreak of the COVID-19 pandemic, the *Lancet* reported that rates of COVID-19 positivity were 5–7 times higher among e-cigarette users than among e-cigarette non-users [6]. Some researches have shown that COVID-19 infection rates and severity are unrelated to using e-cigarettes [7]. Furthermore, the infection and inflammatory response associated with SARS-CoV-2 can differ depending on whether nicotine or flavoring is used in the e-cigarette [8,9]. Retrospective studies have indicated that compared to non-smokers, the risk of e-cigarette and traditional cigarette users developing cardiovascular and metabolic disorders is similar. However, in terms of asthma, COPD, and oral diseases, the risk of e-cigarette users developing these conditions is lower than that of traditional cigarette users, but still significantly higher than non-smokers. Additionally, dual users, who use both e-cigarettes and traditional cigarettes, have a 20 %–40 % higher chance of developing diseases compared to traditional cigarettes users [10]. Thus, multiple lines of clinical evidence suggest the risk of e-cigarette use remains incompletely understood.

As a protective barrier, the bronchial epithelium is composed of ciliated cells, goblet cells, club cells, and basal cells, which cooperate with each other and contribute to airway homeostasis. The beating of ciliated cells and secretion of mucus by goblet cells are critical for epithelial mucociliary clearance function, which is responsible for propelling inhaled pathogens and other harmful particles out of the airway [11]. Basal cells are multipotent progenitor-like cells that play an important role in proliferation and repair of the airway epithelium [12]. Club cells are secretory cells that also function as progenitor cells [12,13]. Damage to the bronchial epithelium can lead to airway inflammation, obstructive pulmonary ventilation, and interstitial hyperplasia, which are related to serious airway diseases such as chronic obstructive pulmonary disease, and pulmonary fibrosis [14,15]. In recent years, more and more studies have focused on the damage that e-cigarette use causes in the airway epithelium, which results in adverse consequences including gas exchange disturbance, immune imbalance, airway inflammation, and epithelium injury [1,16]. However, the cell type-specific effects of e-cigarette use and their underlying molecular mechanisms in the bronchial epithelium have not been adequately studied.

Bulk transcriptomic analyses have described e-cigarette-induced changes in epithelial gene expression [9,17]; however, bulk RNA sequencing masks the contributions and alterations of individual cell types. Single-cell RNA sequencing (scRNA-seq) allows profiling of transcriptional differences, lineage relationships, and responses in individual bronchial epithelial cell types with single-cell resolution, but recent studies have mainly focused on the effects of conventional cigarettes rather than e-cigarettes [18]. Air-liquid interface (ALI) culture is an *in vitro* method that simulates the biological characteristics of normal airway epithelium by enabling primary airway epithelial cells to differentiate into several cell types with pseudo-multi-layered structure and mucous secretion capability [19]. The ALI model has been widely used to study the etiology, pathology, and potential therapeutic targets of human respiratory diseases [19–21]. In the present study, we used multiplex scRNA-seq to study the effects of e-cigarette aerosol on the transcriptional landscape of ALI-cultured human bronchial epithelium. Our results provide new insights into cell type-specific responses to e-cigarette use and will contribute to the search for strategies to counteract e-cigarette-associated respiratory pathologies.

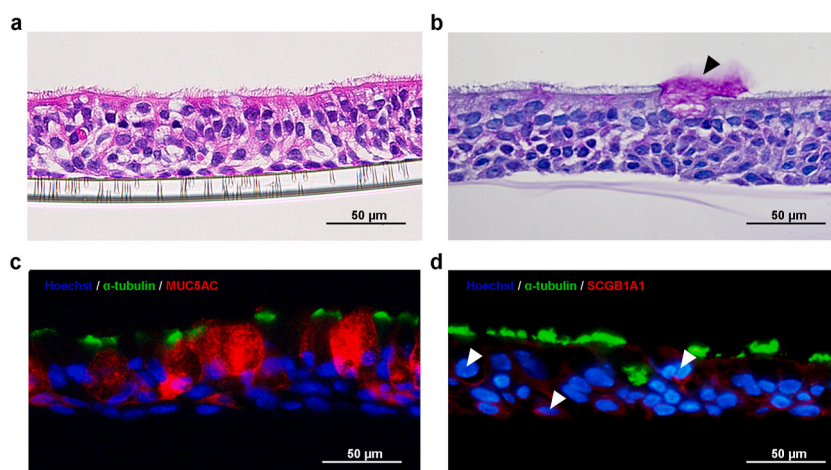


**Fig. 1.** Characterization of mucociliary ALI-HBE. (a) H&E staining and (b) PAS staining (black arrow pointed) showed the mucociliary pseudostratified structure of ALI-HBE. Immunofluorescence showed cell-specific markers of (c) ciliated cells ( $\alpha$ -tubulin, green) and goblet cells (MUC5AC, red) and (d) ciliated cells ( $\alpha$ -tubulin, green) and club cells (SCGB1A1, red, white arrow pointed), both with nuclear counterstain (Hoechst, blue). Scale bars equal 50  $\mu$ m.

2. Results

2.1. Single-cell transcriptome analysis revealed the heterogeneity of ALI-HBE

Primary HBECs were induced by ALI culture to differentiate into ALI-HBE, which is a pseudostratified bronchial epithelium consisting of ciliated cells, secretory cells (goblet cells and club cells), and basal cells (Fig. 1). The ciliated cells and goblet cells are located on the apical side (exposed to the air) of the ALI-HBE, whereas basal cells are located on the basolateral side (submerged in the liquid culture medium).

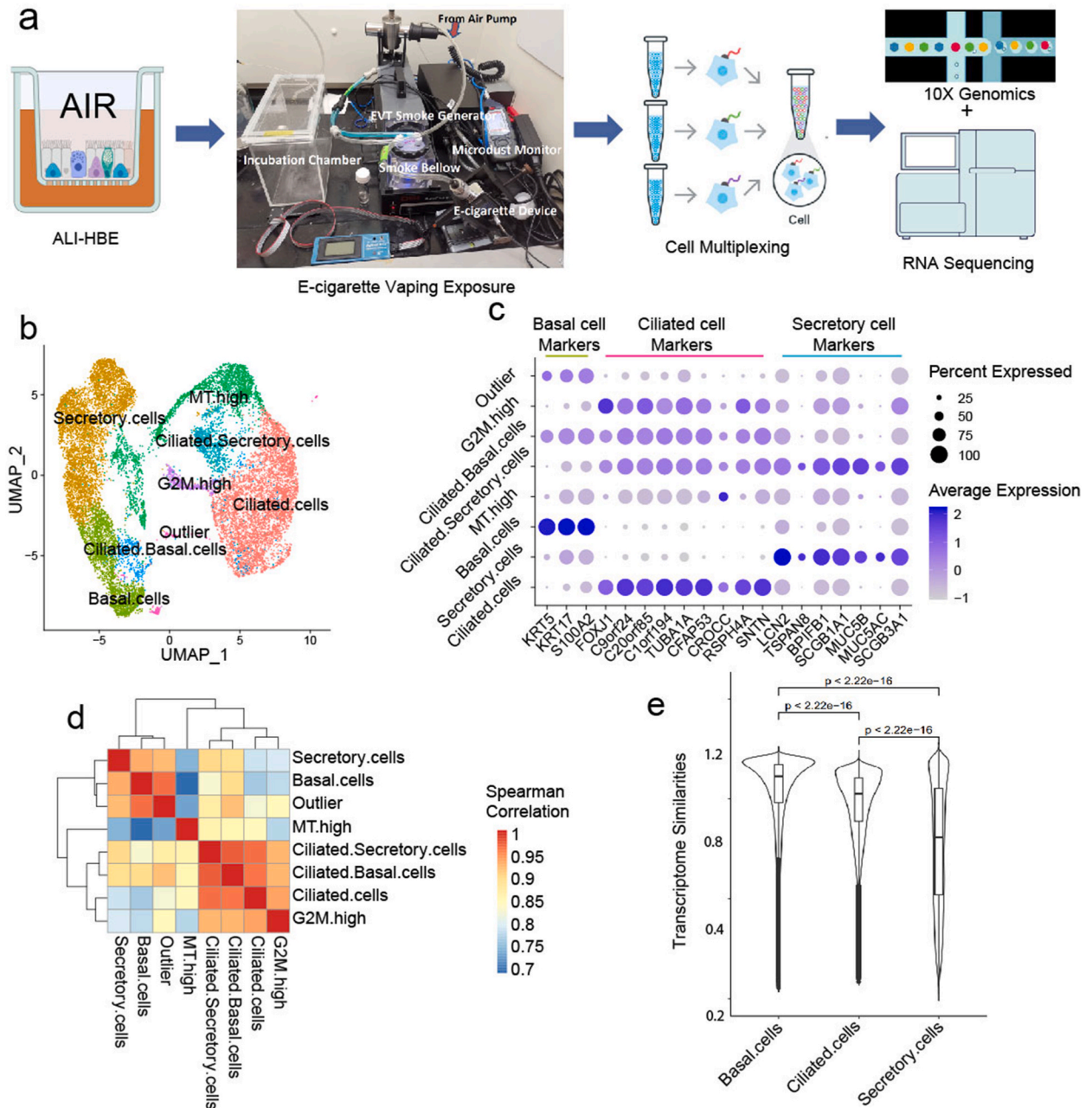


**Fig. 2.** Single-cell transcriptome analysis revealed the heterogeneity of ALI-HBE. (a) A schematic of the experimental design and procedure to investigate the impact of acute exposure to e-aerosol on ALI-HBE. (b) UMAP visualization of the total cells resolved by single-cell sequencing, colored by cell types. (c) Expression of canonical cell markers expression in all cell types. (d) Transcriptome similarities between cell types estimated by Spearman correlation. (e) Violin and boxplot of transcriptome similarities within cell types. BC: basal cell; SC: secretory cell; CC: ciliated cell; CSC: ciliated secretory cell; CBC: ciliated basal cell; Ni: nicotine; Flav: flavoring.

The effects of common e-liquid ingredients were evaluated independently by exposing fully differentiated ALI-HBE to e-aerosol. The commercially available flavored refill fluid (the term “flavoring” will be used to refer to it in the following text) used in the current study was from Saucy contains ~65 % propylene glycol (PG), ~35 % vegetable glycerine (VG) as solvent, food flavoring and menthol. Thus, a vehicle control was prepared using 65 % PG and 35 % VG. To further explore the effects of nicotine on bronchial epithelium, the nicotine liquid was added to the vehicle control or Saucy e-liquid. The types of e-liquid on the market are diverse, such as those containing only flavor, those containing only nicotine, or those containing both, so in order to analyze the effects of different components in e-liquid on the airway epithelial transcriptome, we set the following exposure conditions based on different types of e-cigarettes: (1) Control: PG/VG (+) Nicotine (-), Flavor (-); (2) Nicotine: PG/VG (+), Nicotine (+), Flavor (-); (3) Flavoring: PG/VG (+); Nicotine (-), Flavor (+); (4) Ni in Flav: PG/VG (+), Nicotine (+), Flavor (+). The ALI cultures were subsequently digested into single-cell suspensions and subjected to multiplex scRNA-seq (Fig. 2a). A total of 15874 effective cells were collected to evaluate the cellular heterogeneity of ALI-HBE and its transcriptomic responses to e-aerosol. Among these, eight distinct clusters were identified by unsupervised cluster analysis (Fig. 2b). Cell type was manual annotated based on known marker genes, which were listed in Fig. 2c. Three predominant cell types were identified by their corresponding marker genes, including basal cells, secretory cells, and ciliated cells (Fig. 2c and Figure S1). Dying and proliferating cells were also identified by high expression of mitochondrial genes (MT high cells) and mitosis-related genes (G2M high cells), respectively. In addition, two small groups of cells were found co-expressing markers of ciliated cells and basal cells (ciliated basal cells, CBCs) or ciliated cells and secretory cells (ciliated secretory cells, CSCs). Comparisons among the cell types revealed that the transcriptomes of basal cells and secretory cells were similar to each other and relatively distinct from the transcriptome of ciliated cells (Fig. 2d). Additionally, comparisons within cell types showed that transcriptome similarity was lowest among the secretory cells and highest among the basal cells (Fig. 2e), suggesting that the secretory cells possessed higher heterogeneity.

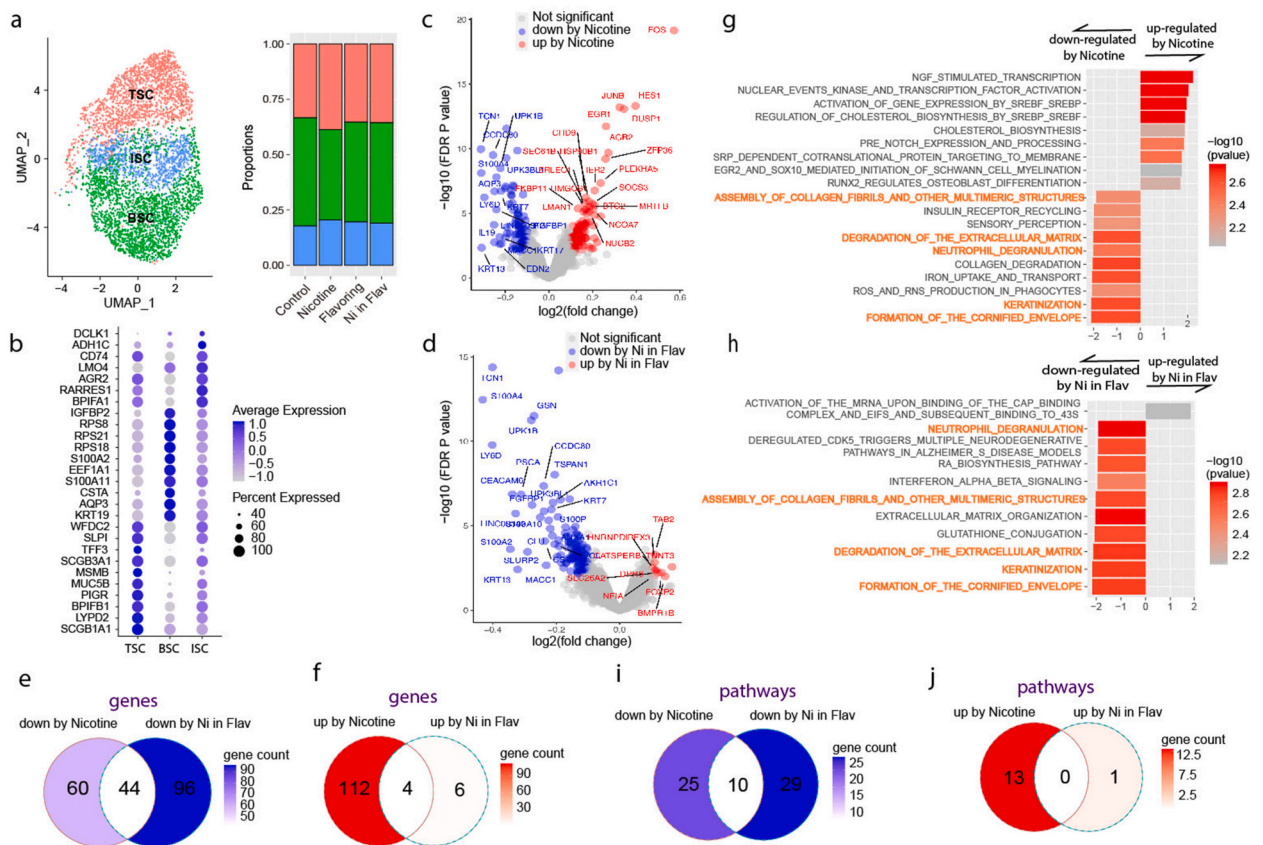


**Fig. 3.** Secretory cell heterogeneity. (a) UMAP visualization of secretory cell clusters (left) and a histogram showing the proportions of the clusters in each sample (right). (b) Dotplot of cell marker expression in the three clusters. (c, d) Volcano plots of differentially expressed genes in secretory cells exposed to nicotine e-aerosol with or without flavoring. (e) Venn diagram showing the overlap of down-regulated genes after exposure to nicotine e-aerosol with or without flavoring. (f) Venn diagram showing the overlap of up-regulated genes after exposure to nicotine e-aerosol with or without flavoring. (g, h) Barplots of differentially expressed gene enrichment on GO biological processes in secretory cells exposed to nicotine e-aerosol with or without flavoring. Shared biological processes are highlighted. (i) Venn diagram showing the overlap of down-regulated pathways after exposure to nicotine e-aerosol with or without flavoring. (j) Venn diagram showing the overlap of up-regulated genes after exposure to nicotine e-aerosol with or without flavoring.

BSC: basal-like secretory cell; TSC: terminal secretory cell; ISC: intermediate secretory cell; Ni: nicotine, Flav: flavoring.

2.2. Acute exposure to nicotine e-aerosol affected gene expression related to secretory cell differentiation and secretion

To further elucidate secretory cell heterogeneity and transcriptional changes after exposure to e-aerosol, we analyzed the transcriptomes of 4857 secretory cells separately, which revealed three main clusters (Fig. 3a, left). The proportions of each cluster of secretory cells were relatively stable across samples (Fig. 3a, right). Basal-like secretory cells (BSCs) were identified by higher expression of basal cell markers (*S100A2* and *KRT19*) and lower expression of secretory cell markers (*MUC5B* and *SCGB3A1*), whereas terminal secretory cells (TSCs) showed the opposite pattern (Fig. 3b). Another distinct cluster, which we named intermediate secretory cells (ISCs), expressed both basal and secretory marker genes.

Next, we performed a differential expression analysis to elucidate potential effects of exposure to nicotine e-aerosol with or without flavoring on secretory cells. Exposure to nicotine e-aerosol without flavoring resulted in upregulation of 116 genes and downregulation of 104 genes relative to the expression levels in cells exposed to vehicle control without nicotine (Fig. 3c). Exposure to nicotine e-aerosol with flavoring resulted in fewer (10) up-regulated genes and more (140) down-regulated genes compared with exposure to nicotine e-aerosol without flavoring (Fig. 3d), suggesting that the influence of nicotine on secretory cells might be different under conditions of distinct flavoring. Forty-four genes were significantly co-down-regulated after exposure to nicotine e-aerosol with or without flavoring. Among these, eight genes were involved in epithelial cell differentiation (*AKR1C1*, *AKR1C2*, *CTSB*, *DHRS9*, *LGALS3*, *GSTK1*, *KRT13*, and *UPK1B*), and six genes were involved in calcium ion binding (*S100A10*, *S100A14*, *S100A4*, *S100A6*, *GSN*, and *TKT*). Notably, among the co-down-regulated genes, 21 genes (51.1 %) were related to extracellular exosomes, and 13 (28.9 %) were secreted proteins, suggesting that nicotine might impair the secretory function of human airway epithelium. Differential expression

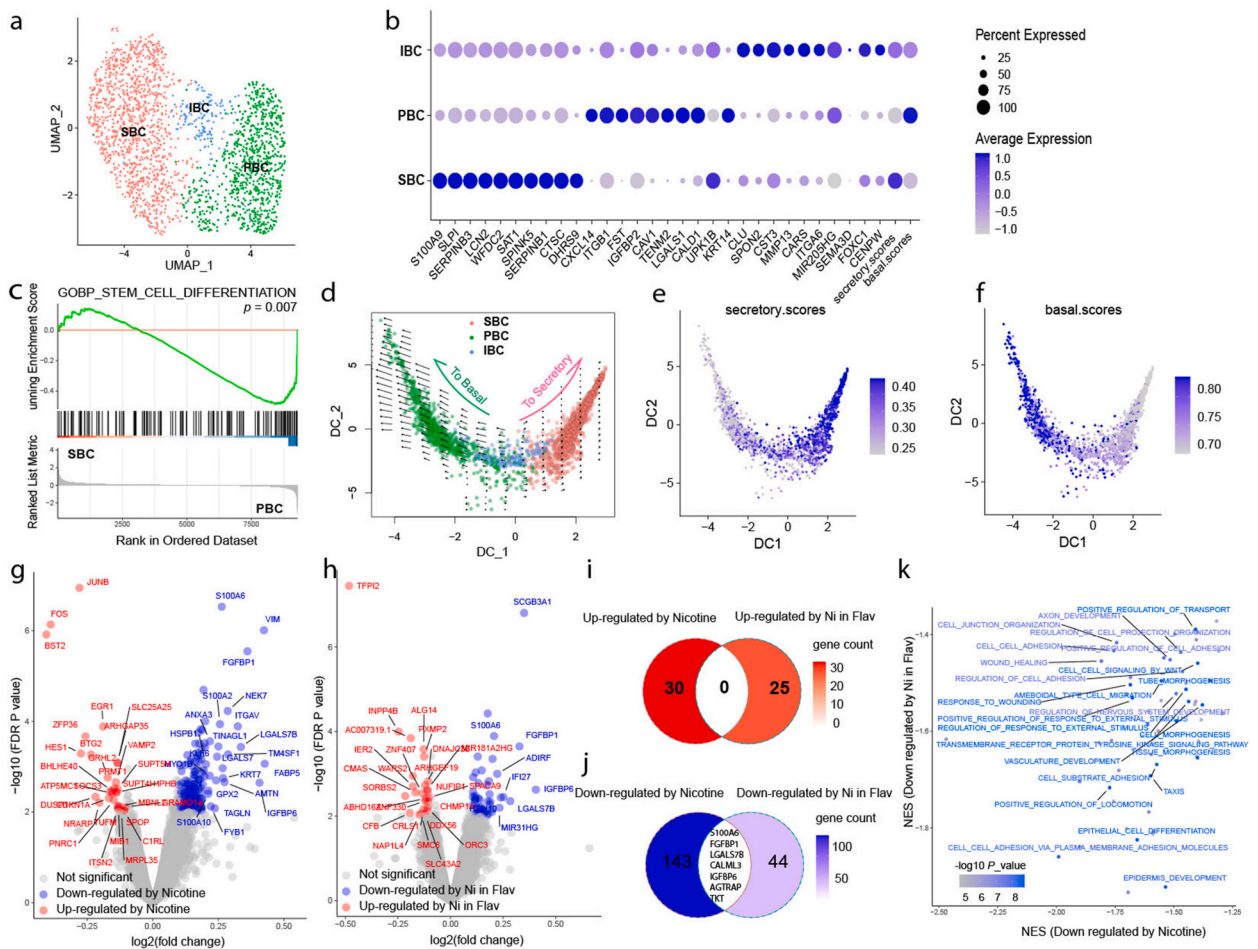


**Fig. 4.** Acute exposure to nicotine e-aerosol promoted basal-to-secretory transformation. (a) UMAP visualization of secretory cell subgroups. (b) Dotplot of marker gene expression in the basal cell subgroups. (c) Gene set enrichment of the cell differentiation biological process in SBCs and PBCs. (d) Cell RNA velocity displayed on a diffusion map. (e) Secretory and (f) basal cell scores displayed on a diffusion map. (g, h) Volcano plot of differentially expressed genes in basal cells after exposure to nicotine e-aerosol (h) without or (g) with flavoring. (i, j) Venn diagram showing the overlap of up-regulated and down-regulated genes after exposure to nicotine e-aerosol with or without flavoring. (k) Dotplot showing significantly co-down-regulated gene sets after exposure to nicotine e-aerosol with or without flavoring. SBC: secretory-like basal cell; PBC: progenitor-like basal cell; IBC: intermediate basal cell; Ni: nicotine; Flav: flavoring.

tests were also performed separately for each of the three main clusters of secretory cells (Figure S2). Fourteen genes were co-upregulated in all three clusters by exposure to nicotine e-aerosol without flavoring, most of which were related to stress response. On the other hand, the genes that were co-down-regulated in all three clusters by exposure to nicotine e-aerosol were similar with or without flavoring. To better supplement and support our findings, we analyzed another published dataset (GSE199072), and we found that secretory cells were the most affected subgroup of cells. Most of the 44 genes down-regulated after nicotine exposure were also down-regulated according to the gene set enrichment analysis (Figure S3).

Pathway enrichment analysis revealed that exposure to nicotine e-aerosol with or without flavoring resulted in downregulation of similar pathways (Fig. 3g–j), such as formation of cornified envelope, keratinization degradation of extracellular matrix, assembly of collagen fibrils and other multimeric structures, and neutrophil degranulation, which might be related to the differentiation and secretory function of the cells [22]. Consistent with the observations of differentially expressed genes, more pathways were down-regulated than were up-regulated after exposure to nicotine e-aerosol, especially in the presence of flavoring, and no gene ontology (GO) biological process was co-enriched by exposure to nicotine e-aerosol with or without flavoring.

### 2.3. Acute exposure to nicotine e-aerosol promoted basal-to-secretory transformation

Next, we analyzed the transcriptomes of 2226 basal cells identified by expression of conventional basal cell markers. Differential expression of specific markers revealed three distinct clusters of basal cells: secretory-like basal cells (SBCs), intermediate basal cells (IBCs), and progenitor-like basal cells (PBCs; Fig. 4a and b). SBCs displayed relatively high secretory scores, estimated by the expression of secretory cell markers (*LCN2*, *TSPAN8*, *BPIFB1*, and *SCGB1A1*). In addition, SBCs showed high expression of *S100A9*, *SLPI*, and *SERPINB3*, which were also highly expressed in secretory cells (Fig. 4b and Figure S4). These top marker genes were highly related to epithelial cell differentiation, and the gene set for this process was enriched in SBCs (Figure S5a, GO:0030855, GSEA  $p = 0.004$ ). These observations suggested that SBCs were likely to initialize differentiation from basal cells to secretory cells and had begun to show secretory characters, such as the biological process of secretion by tissue (Figure S5b, GO:0032941, GSEA  $p = 0.005$ ).

Compared with SBCs, PBCs expressed much higher levels of TP63 (Figure S5c), a traditional epithelial basal cell marker, and also presented a high level of progenitor cell regulation. GSEA results showed that PBCs were enriched with expression of genes involved in stem cell differentiation (Fig. 4c, GO:0048863, GSEA  $p = 0.007$ ). They were also relatively highly enriched with expression of biological processes involved in cell adhesion, cell matrix, fiber assembly and substrate junction, and external encapsulating structure organization (Figure S5f), indicating that the stemness of basal cells plays important roles in maintaining the structure and environment of bronchial epithelium in the ALI model. Additionally, PBCs were enriched with expression of transforming growth factor beta (*TGFB*) production pathways (Figure S5d and S5e), suggesting they might be involved in cell proliferation, differentiation, and growth. IBCs expressed marker genes of both SBCs and PBCs and showed intermediate levels of secretory and basal scores, suggesting they were in an intermediate state between the other two basal subtypes.

Pseudotime analysis was performed on basal cells (Fig. 4d–f) using diffusion map algorithm (R, package *Destiny*, v3.2.0). On this basis, RNA velocity was applied to determine the direction of cell development which is indicated by arrows (R, package *Velocyto* v0.6). Combined with RNA velocity analysis, the trajectory could be divided into two directions. One represented the basal-to-secretory transition, which was mostly occupied by SBCs with high secretory scores (Fig. 4e). The other branch, which was mostly occupied by PBCs, had higher basal scores (Fig. 4f) and represented basal cells shifting into a stem/progenitor-like status to maintain renewal and proliferation potential.

Differential expression analysis revealed a series of genes that were significantly up-regulated or down-regulated after exposure to nicotine e-aerosol (Fig. 4g and h). Among the up-regulated genes, bone marrow stromal cell antigen 2 (*BST2*) belongs to the IFN-stimulated genes (*ISGs*) family, which is a limited gene set that controls viral infection by inhibiting viral RNA synthesis, viral assembly/egress, and viral entry. In addition, *FOS* and *JUNB* are the key members forming the transcription factor complex AP-1, which is related to basal-to-squamous cell carcinoma transition [23]. Similar to the observation in secretory cells, no genes were co-up-regulated after exposure to nicotine e-aerosol with or without flavoring, suggesting that the influence of nicotine on basal cells might be different under conditions of distinct flavoring (Fig. 4i). Nevertheless, seven genes were co-down-regulated after exposure to nicotine e-aerosol with or without flavoring (Fig. 4j). Three of these genes were involved in negative regulation of cell proliferation (DAVID, GO: 0008285,  $p = 0.016$ ), suggesting that nicotine might promote basal cell proliferation (especially in SBCs) by down-regulating genes that inhibit cell growth, which is consistent with the observation that nicotine may promote basal-to-secretory transition. Furthermore, a series of biological functions were co-down-regulated by exposure to nicotine e-aerosol with or without flavoring (Fig. 4k), including genes involved in stimulus responses, cell communication, cell development, and wound healing.

### 2.4. Acute exposure to nicotine e-aerosol with flavoring might promote susceptibility to virus infection

In addition to nicotine, the effects of flavoring were investigated (Figure S6). Several genes were differentially expressed after acute exposure to e-aerosol with flavoring with or without nicotine. Among these, five genes were involved in cytokine signaling in immune response (*FOS*, *JUNB*, *SOC3*, *IFI27*, and *BST2*; Fig. 5a–d). However, the number of genes that were up-regulated by exposure to e-aerosol with flavoring was diminished in the presence of nicotine (Fig. 5c). These observations suggested that nicotine might affect how epithelial cells respond to the flavorings. Interestingly, in basal cells, many genes were up-regulated but only a few were down-regulated after exposure to e-aerosol with flavoring, whereas ciliated cells showed the opposite pattern (Fig. 5a–d), suggesting that different types of epithelial cells might react distinctly to e-aerosol flavoring. To better understand the pathways impacted by the flavoring, we identified significant differentially expressed genes using STRING databases and generated an interaction network



**Fig. 5.** Acute exposure to e-aerosol with flavoring might contribute to virus infection susceptibility. (a–d) Venn diagrams displaying (a, c) co-up-regulated and (b, d) co-down-regulated genes in three predominant cell types after exposure to e-aerosol with flavoring with or without nicotine. (e) The gene network constructed with significantly co-regulated genes and their highly interacting genes from STRING. The node color represents the fold change between vehicle control and samples with flavoring; the size represents p values. (f) Dotplot visualizing the expression of genes related to SARS-CoV infection. (g, h) Gene set enrichment plots showing significantly enriched pathways related to SARS-CoV infection in basal cells exposed to e-aerosol with flavoring (h) with or (g) without nicotine.

BC: basal cell; SC: secretory cell; CC: ciliated cell; Ni: nicotine; Flav: flavoring.

(Fig. 5e). Exposure to e-aerosol with flavoring increased expression of genes that interact with genes from the MAPK (*MAPK9*, *MAPK8*, *MAPK14*, *MAPKAPK2*) and JAK-STAT (*JAK2* and *EPOR*) pathways, which might trigger the expression of a wide array of cytokines and growth factors to promote cell differentiation and growth. In addition, the same exposure down-regulated the genes *BST2* and *IFI27*, which interact with the early growth response protein *EGRI*, further suggesting that the growth pattern of epithelial cells was switched in the presence of e-aerosol flavoring.

To further investigate the potential connection between e-cigarette use and virus infection, we investigated five of the most relevant genes in SARS-CoV-2 infection (*ACE2*, *TMPRSS4*, *TMPRSS2*, *CTSL*, and *BSG*). The expression of *ACE2*, the receptor for the spike glycoprotein of human coronavirus, was increased in basal cells after exposure to e-aerosol with flavoring (Fig. 5f), suggesting that bronchial epithelial basal cells might be more susceptible to SARS-CoV infection after exposure to e-aerosol containing flavoring. In line with this observation, expression of a series of pathways related to SARS-CoV infection was enriched in ALI-HBE basal cells after exposure to e-aerosol with flavoring regardless of whether the e-aerosol contained nicotine (Fig. 5g and h).

### 2.5. Acute exposure to e-aerosol affected epithelial cell interactions

To investigate how the ALI-HBE cells communicate with each other, we constructed cell-to-cell interaction networks based on ligand-receptor pair databases (Fig. 6a). We found that basal cells, especially PBCs and IBCs, which possess high stemness potential, were more likely than other cell types to interact with each other and with other cell types (Fig. 6b and c). In addition, PBCs and IBCs were the most self-regulating cells in the ALI culture system, suggesting that they might possess higher potential to adjust to the growth environment. Comparatively, secretory cells showed less participation in cell communication, and ciliated cells showed the least evidence of intracellular communication.

The top four pathways through which basal cells interacted with other basal cells were the MK, LAMININ, MIF, and COLLAGEN pathways (Fig. 6d). In the ALI-HBE model, MIF interacted strongly with ACKR3 and the CD74 and CD44 complex (Figure S7c). The main interactions enriched in secretory cells included the MK, PTN, and EPHA pathways (Fig. 5d; Figure S7a and S7e). MK was also the most extensively interacting pathway in the entire ALI-HBE.

Next, we compared changes in bronchial epithelial cell interactions after acute exposure to e-aerosol. The results showed that exposure to nicotine e-aerosol without flavoring had a significant effect on cell interactions, which enhanced the ability of secretory cells to secrete signals, whereas PBCs were the least affected (Fig. 6e; Figure S8a). An analysis of signaling pathways showed that the EGF pathway was the most altered pathway after exposure to nicotine e-aerosol without flavoring (Fig. 6f; Figure S8b). In the presence of flavoring, the ability of most cell types to express and receive signals after exposure to nicotine e-aerosol was reduced, and the CDH and JAM pathways were significantly inhibited (Fig. 6e–h).

## 3. Discussion

Previous studies have shown the negative effects of e-cigarettes on the airway epithelium by concentrating on immune responses and lung pathology [24–26]. Some recent studies have explored the potential molecular mechanisms of the overall effects at the transcriptome level through bulk RNA sequencing. However, exploring the effects at the single-cell level can observe cell type-specific transcriptome changes, but also their interactions. By bulk RNA sequencing, researchers have found that e-cigarettes affect the function of airway epithelium by increasing oxidative stress, inhibiting cilia production, and maintaining inflammatory responses, and may contribute to airway disease progression [27,28]. These two studies have highlighted the effects of e-cigarettes on ciliated cells, however, the effects on other cell types of bronchial epithelium are unknown. We examined this at single-cell resolution and have found that e-cigarettes have significant effects on secretory cells and basal cells as well, including inhibition of secretory function, increasing the susceptibility of basal cells to SARS-CoV, and altering epithelial cell interactions. Besides, studies have shown that e-cigarettes containing nicotine and flavorings can cause significant cytokine dysregulation and inflammasome activation in airway epithelial cells [9,29,30], which may be closely related to a series of transcriptomic changes found in our research.

A total of eight cell clusters covering the known bronchial epithelium cell types (basal, secretory, ciliated, and intermediate cells) were identified by multiplex scRNA-seq, suggesting that the primary traits of human bronchial epithelial communities were mirrored in the ALI-HBE cultures. Additionally, our results identified novel marker genes and sub-population heterogeneity in human bronchial epithelium. The highest transcriptional heterogeneity occurred in secretory cells, which could be divided into BSCs, TSCs, and ISCs according to the RNA expression levels of marker genes. Club cells are considered to be one of the major progenitors of the airway epithelium, having the ability of self-renewal and further differentiation into other cell types (e.g. goblet cells and ciliated cells), which plays an important role in maintaining the integrity and repairing injury of the airway epithelium [31]. On the other hand, goblet cells are characterized by their “flask-shaped” morphology and production of mucus that reacts with PAS staining [32]. During epithelial differentiation, club cells continue to differentiate into goblet cells, which was reflected in our single-cell sequencing results as a

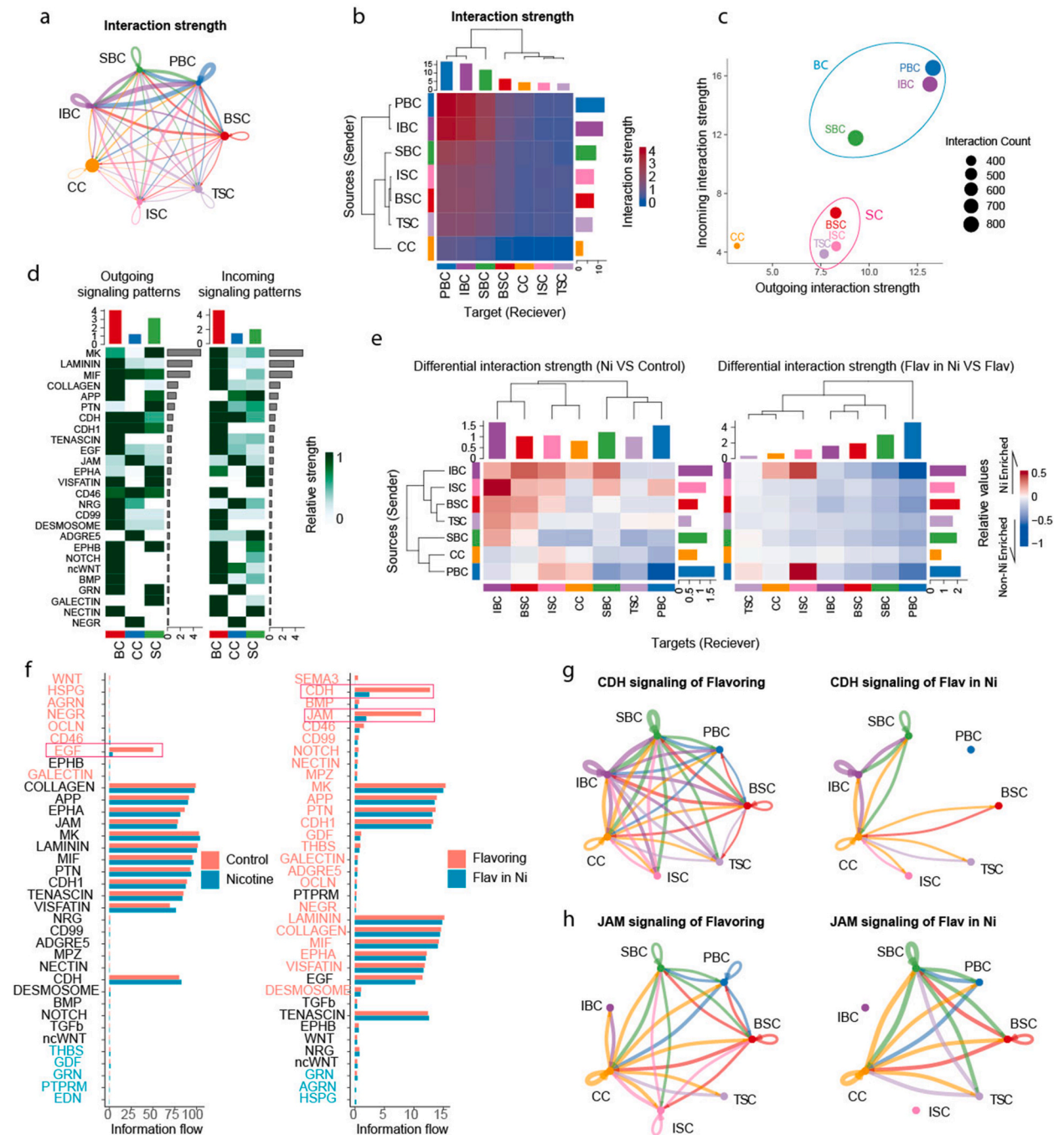


**Fig. 6.** Epithelial cell interactions. (a) Circle plot of the cell interaction network. (b) Heatmap displaying cell interactions. (c) Dot plot showing the interaction roles of each cell type. (d) Heatmap displaying outgoing and incoming signaling patterns. (e) Heatmap displaying differential interaction strength after exposure to nicotine e-aerosol with or without flavoring. (f) Bar plot comparing pathway expression changes after exposure to e-aerosol with flavoring with or without nicotine. (g) CDH signaling interaction networks. (h) JAM signaling interaction networks. CC: ciliated cell; SC: secretory cell; BC: basal cell; BSC: basal-like secretory cell; TSC: terminal secretory cell; ISC: intermediate secretory cell; SBC: secretory-like basal cell; PBC: progenitor-like basal cell; IBC: intermediate basal cell; ISC: intermediate secretory cell; Ni: nicotine; Flav: flavoring.

transition from BSCs to TSCs. According to our histological results and previous reports, goblet cells and club cells can be clearly distinguished by their cell morphology and expression of marker proteins such as *MUC5AC* and *SCGB1A1* [33,34]. However, these two cell types cannot be distinguished at the transcriptome level by their marker proteins [35–37]. It has been established that detrimental stimuli cause bronchial goblet cell hyperplasia and persistent mucin production. This is linked to a variety of pathological conditions,

such as airway infection and obstruction [38,39]. The more adaptable and dynamic post-transcriptional regulation of goblet cells and club cells perfectly matches the functional needs of the elastic response of the airway epithelium to different types of stimuli.

We performed cell interaction analyses to explore the effects of e-aerosol on signal communication among the heterogeneous bronchial epithelial cells. MK, one of the top four cell interaction pathways of basal cells, is a heparin-binding growth factor, whereas EPHA proteins are associated with epithelial cell permeability [40]. Another one, MIF could be found in various cell types and has been shown to activate a series of downstream pathways, including the ERK1/2, AMPK, and AKT pathways, via autocrine and paracrine signals to exert the function of epithelial repair [41]. LAMININ and COLLAGEN proteins are major contributors to extracellular matrix formation and structural organization [42]. The enrichment of such interactions in basal cells is in line with the functions of basal cells in anchoring the epithelium to the basement membrane. Acute exposure to nicotine e-aerosol had a significant effect on cell interactions that enhanced the abilities of secretory cells to express signals and intermediate cells to receive signals, which suggests that secretory cells may play a role in regulating the cell fate of intermediate cells. Basal cells were the least affected by exposure to nicotine e-aerosol, suggesting that these cells are crucial for maintaining repair potential and homeostasis in the airway epithelium. In the presence of e-aerosol flavoring, the ability of most cell types to express and receive signals was reduced, and the pathways showing the most pronounced changes were the CDH and JAM pathways, suggesting that the flavoring might activate the epithelial-to-mesenchymal transition and impair epithelial cell tight junctions and physical barrier function [41,43].

Epidemiological findings during the COVID-19 pandemic have shown that e-cigarette use can greatly increase the risk of SARS-CoV-2 infection and related complications [2,44]. Preliminary data suggested that nicotine might upregulate the ACE2 receptor, the site of SARS-CoV-2 entry into cells [6]. Interestingly, an earlier study found that PG/VG and nicotine in e-cigarettes increased airway epithelium susceptibility to SARS-CoV-2 pseudoparticles, but benzoic acid mitigated this effect. In our study, benzoic acid-free e-liquid were used, and we found that flavoring upregulated SARS-CoV-2 susceptibility genes, not nicotine. There may be a variety of reasons for such inconsistent results, including the use of different e-liquid brands and different nicotine doses, or the conditions of aerosol exposure. Whether e-cigarettes increase the susceptibility to SARS-CoV-2 infection and which specific component in e-liquid plays a role is obviously a matter of debate, and more research is required in the future to prove this. Furthermore, among the genes that were differentially expressed after exposure to e-aerosol with flavoring, the expression of *BST2* was significantly inhibited after the exposure, regardless of whether the e-aerosol contained nicotine. *BST2* belongs to the ISGs family, which is a limited gene set that controls viral infection by inhibiting viral RNA synthesis, viral assembly/egress, and viral entry [45]. Recent studies have shown that *BST2* can effectively inhibit SARS-CoV-2 RNA replication and virus release, which suggests it could be a potential therapeutic target [45,46]. We found that acute exposure to e-aerosol with flavoring significantly inhibited *BST2* expression, suggesting a molecular mechanism by which flavored e-cigarette use can promote susceptibility to virus infection, and also providing a potential therapeutic target for vaping-related lung injury. However, it is important to acknowledge that there are thousands of flavors of e-cigarettes on the market today, and the current experiment tested only one of them, and the outcomes may not universally apply to all flavors.

In summary, our results delineate the transcriptional heterogeneity of human bronchial epithelium and cell (sub)type-specific responses to e-aerosol containing nicotine and/or flavoring at the single-cell level. Nicotine or e-aerosol flavoring may cause changes in cell differentiation, secretory function, and susceptibility to viral infection of the bronchial epithelium (Fig. 7). These findings emphasize the need for more research into the safety and toxicity of e-cigarette use and provide insights for the development of cell-specific treatments.

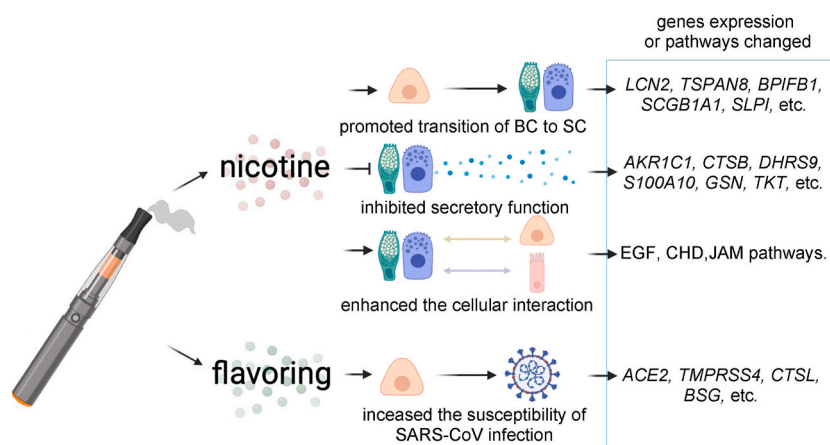


**Fig. 7.** Schematic summary of the effects of acute exposure to e-aerosol on human bronchial epithelial transcriptome. The findings of our study show that nicotine-containing e-aerosol affected gene expression related to transformed basal cells into secretory cells after acute exposure; inhibition of secretory cell function by down-regulating genes related to epithelial cell differentiation, calcium ion binding, extracellular exosomes, and secreted proteins; and enhanced interaction between secretory cells and other cells. On the other hand, flavoring may alter the growth pattern of epithelial cells and make basal cells more susceptible to SARS-CoV infection. Besides, the data also indicate factors that may promote SARS-CoV-2 infection and suggest therapeutic targets for restoring normal bronchial epithelium function after e-cigarette use.

#### 4. Limitations of the study

Some limitations of our study should be noted. First, real-world smokers experience cumulative effects from e-cigarettes over time on their airway epithelium. Accordingly, the conclusions drawn from this study based on acute exposure to an *in vitro* ALI model are limited. Future studies should establish experimental methods of chronic exposure to e-cigarettes and use airway epithelium samples obtained from real smokers to examine long-term effects. Second, the flavoring tested in this study were of a single source, the changes caused by flavoring exposure do not apply to the flavors of all currently available e-cigarettes. Third, the experimental data obtained from a single donor-derived primary cells may not be representative and reproducible, which required a larger sample size in the future study. Finally, the ALI-HBE model used in this study mimicked the structure and physiological function of human bronchial epithelium to a certain extent, but the experimental data and conclusions based on the above *in vitro* experiments need to be further verified by *in vivo* experiments.

#### 5. Resource availability

##### 5.1. Lead contact

Further information and requests for resources and reagents should be directed to and will be fulfilled by the lead contact, Wing-Hung Ko ([whko@cuhk.edu.hk](mailto:whko@cuhk.edu.hk)).

##### 5.2. Experimental model and subject details

###### 5.2.1. ALI-HBE (air-liquid interface cultured human bronchial epithelium) model

ALI culture was used to induce differentiation of primary human bronchial epithelial cells (HBECs) into bronchial epithelium as described in our previous study [33]. Briefly, commercial primary HBECs (ScienCell, Cat#3210, Lot#6457, Carlsbad, CA, USA) from a single healthy donor were submerged in PneumaCult-Ex Plus Expansion Medium (StemCell, Tukwila WA) in a T25 flask. Expanded HBECs were then sub-cultured and seeded on six-well plates with poly-L-Lysine-coated Transwell inserts (0.4  $\mu\text{m}$  pore size; Costar, Cambridge, MA), and expansion medium was applied to the apical and basolateral chambers. When a monolayer of HBECs formed, ALI culture was performed by removing the apical medium and replacing the basolateral medium with PneumaCult-ALI Maintenance Medium to induce HBEC differentiation into polarized bronchial epithelium within 28 days.

#### 6. Method details

##### 6.1. Histological staining

On day 28 of ALI culture, epithelium was harvested for histological staining as described previously [33]. Briefly, ALI cultures were fixed in 4 % paraformaldehyde followed by agar-paraffin embedding. Five-micrometer de-paraffinized sections were subjected to hematoxylin & eosin (H&E) or period acid–Schiff (PAS) staining or to antigen retrieval followed by immunofluorescence staining. For immunofluorescence staining, primary antibodies,  $\alpha$ tubulin (sigma, 1:1000), SCGB1A1 (ABclonal, 1:100) were incubated with the ALI sections at 4 °C overnight, followed by incubating with secondary antibody (Alexa Flour-488 conjugated and Alexa Flour-647 conjugated, Invitrogen, 1:1000) and MUC5AC (Alexa Fluor-594 conjugated, abcam, 1:100) at room temperature for 1 h. Sections were counterstained with Hoechst after wash. Images were acquired using an Olympus IX83 Inverted Microscope (Olympus, Tokyo, Japan).

##### 6.2. Exposure of ALI-HBECs to e-aerosol

ALI-HBECs were put into an induction chamber (24  $\times$  12  $\times$  18 cm; RWD Life Science, Guangdong, China) and exposed to e-aerosol using a Buxco Smoke Generation and Delivery System (Data Sciences International, MN, USA) as described by Manevski et al. [47]. In this system, an electrically powered e-cigarette device (SMOK® X-Priv, Shenzhen IVPS Technology, SZ, PRC) generates e-aerosol at 70 W. The system was also connected to an aerosol concentration measurement instrument (MicroDust Pro, Casella, Bedford, UK). Real-time monitoring of the total particulate matter (TPM) concentration generated by the vaping protocol of the smoking machine was performed before the e-vapor was delivered to the cultured cells inside the chamber. It was found that the TPM generated at 70 W was relatively constant at  $833.3 \pm 65.3$  mg/m<sup>3</sup>, n = 6).

The commercial flavored refill fluid used in the current study is SAUCY Pomme Kiwi Zero Degrees e-liquid (Los Angeles, CA, USA, <http://saucygroup.com/>). According to the bottle description, which contains ~65 % propylene glycol (PG), ~35 % vegetable glycerine (VG) as solvent and flavored with Kiwi fruit, apple, and menthol. Thus, a vehicle control was prepared using 65 % PG and 35 % VG. 20 mg/ml of nicotine liquid ( $\geq 99$  % (GC, from Sigma-Aldrich, #N3876, MO, USA) was added to vehicle control or Saucy e-liquid. The e-aerosol was delivered in cycles using the high-puff volume and frequency protocol developed by Anthérieu et al., with each cycle consisting of a 55 ml puff drawn over 3 s [48]. Each day for three consecutive days, HBECs were exposed to 12 cycles of e-aerosol at 30 s intervals.

### 6.3. Multiplex scRNA-seq

After e-vapor exposure, ALI cultures were washed with warm PBS followed by using apical dissociation solution (Accutase with 5 mM EDTA and 5 mM EGTA) for 30 min at 37 °C with occasional manual agitation. Then 40 µM Cell strainers were used to harvest live singlets. A cDNA library was then prepared using Chromium Next GEM Single Cell 3' Reagent Kits v3.1, dual index with Cell Multiplexing Oligo Labeling. Briefly, the harvested cells were washed and quantified using a Countess II FL Automated Cell Counter, and a total of  $1 \times 10^6$  live cells from each group were labeled with Cell Multiplexing Oligos. A Gel-bead-in-emulsion was generated by combining Master Mix containing oligo-labeled cells, barcoded Single Cell 3' Gel Beads, and Partitioning Oil on a Next GEM Chromium Chip G. Then,  $10 \times$  Barcoded cDNA molecules were amplified by PCR with compatible primers to generate sufficient mass for library construction. Finally, two libraries (Gene Expression and Cell Multiplexing) were sequenced as 150 base-pair dual-end reads on an Illumina HiSeq 2500 (Illumina, Inc., San Diego, CA).

### 6.4. Data analysis

Single-cell data were analyzed as described in our previous study [49]. Briefly, Cell Ranger (v6.1.0) was used to visualize and create single-cell expression matrices. SCTransform normalization was applied by using 3000 genes as a highly variable gene set, and Seurat (v4.0.4) was used to integrate data from different batches. A total of 15 main components were chosen for UMAP display and cell clustering. Cells were aligned with SingleR (v1.6.1) to BLUEPRINT and ENCODE. Clusters were allocated to cell types based on alignments and established cell markers. The package clusterProfiler (V4.8.0) was used for gene set enrichment analysis (GSEA). The AUCell package (v1.10.0) in R was used to generate gene set scores for customized gene set comparisons across various cell groups. Pseudotime trajectory on UMAP was constructed using Monocle3 (v1.0.0). Additional supporting data were obtained by computing cell differentiation using the diffusion map algorithm (v3.2.0). Cell development directions were estimated using the package Velocity.R (v0.6). CellChat (v1.1.0) combined with built-in curated databases was applied to investigate cell-to-cell interactions. The normalized SCTgene count matrix was used as input to construct interaction networks. Diagrams were created with BioRender.com and figures were created with Adobe Illustrator (Adobe Inc., 2023).

### Data availability

The data presented in the study are deposited in the OMIX repository, accession number OMIX005270.

### CRedit authorship contribution statement

**Meng-yun Cai:** Writing – original draft, Methodology, Investigation, Data curation, Conceptualization. **Xiaofan Mao:** Methodology, Formal analysis. **Beiyang Zhang:** Methodology, Formal analysis. **Chung-Yin Yip:** Methodology, Investigation. **Ke-wu Pan:** Methodology, Investigation. **Ya Niu:** Methodology, Investigation. **Stephen Kwok-Wing Tsui:** Methodology, Investigation. **Joaquim Si-Long Vong:** Methodology, Investigation. **Judith Choi-Wo Mak:** Methodology, Investigation. **Wei Luo:** Writing – review & editing, Supervision, Resources, Project administration, Funding acquisition, Data curation, Conceptualization. **Wing-Hung Ko:** Writing – review & editing, Supervision, Resources, Project administration, Funding acquisition, Data curation, Conceptualization.

### Declaration of competing interest

The authors declare the following financial interests/personal relationships which may be considered as potential competing interests: Wing-Hung Ko reports financial support was provided by Research Grant Council General Research Fund. Wing-Hung Ko reports financial support was provided by Health and Medical Research Fund, Food and Health Bureau, Government of the Hong Kong Special Administrative Region. Xiaofan Mao reports financial support was provided by National Natural Science Foundation of China. If there are other authors, they declare that they have no known competing financial interests or personal relationships that could have appeared to influence the work reported in this paper.

### Acknowledgments

This work was funded by the Research Grant Council General Research Fund (CUHK 14107920) and the Health and Medical Research Fund, Food and Health Bureau, Government of the Hong Kong Special Administrative Region (Project no. 07183806), which were awarded to Wing-hung KO. The study was supported by grants from the National Natural Science Foundation of China (82103347).

### Appendix A. Supplementary data

Supplementary data to this article can be found online at <https://doi.org/10.1016/j.heliyon.2024.e38552>.

## References

- [1] L.F. Chun, F. Moazed, C.S. Calfee, M.A. Matthay, J.E. Gotts, Pulmonary toxicity of e-cigarettes, *Am. J. Physiol. Lung Cell Mol. Physiol.* 313 (2017) L193–L206.
- [2] T. Munzel, O. Hahad, M. Kuntic, J.F. Keaney, J.E. Deanfield, A. Daiber, Effects of tobacco cigarettes, e-cigarettes, and waterpipe smoking on endothelial function and clinical outcomes, *Eur. Heart J.* 41 (2020) 4057–4070.
- [3] K.W. Bold, S. Krishnan-Sarin, C.M. Stoney, E-cigarette use as a potential cardiovascular disease risk behavior, *Am. Psychol.* 73 (2018) 955–967.
- [4] T. Gordon, E. Karey, M.E. Rebuli, Y.H. Escobar, I. Jaspers, L.C. Chen, E-cigarette toxicology, *Annu. Rev. Pharmacol. Toxicol.* 62 (2022) 301–322.
- [5] B.A. King, C.M. Jones, G.T. Baldwin, P.A. Briss, The EVALI and youth vaping epidemics - implications for public health, *N. Engl. J. Med.* 382 (2020) 689–691.
- [6] The Lancet Respiratory M, The EVALI outbreak and vaping in the COVID-19 era, *Lancet Respir. Med.* 8 (2020) 831.
- [7] H. Tattan-Birch, O. Perski, S. Jackson, L. Shahab, R. West, J. Brown, COVID-19, smoking, vaping and quitting: a representative population survey in England, *Addiction* 116 (2021) 1186–1195.
- [8] M. Gao, P. Aveyard, N. Lindson, J. Hartmann-Boyce, P. Watkinson, D. Young, C. Coupland, A.K. Cliff, D. Harrison, D. Gould, et al., Association between smoking, e-cigarette use and severe COVID-19: a cohort study, *Int. J. Epidemiol.* 51 (2022) 1062–1072.
- [9] A.C. Lee, J. Chakladar, W.T. Li, C. Chen, E.Y. Chang, J. Wang-Rodriguez, W.M. Ongkeko, Tobacco, but not nicotine and flavor-less electronic cigarettes, induces ACE2 and immune dysregulation, *Int. J. Mol. Sci.* 21 (2020).
- [10] S.A. Glantz, N. Nguyen, A.L. Oliveira da Silva, Population-based disease odds for E-cigarettes and dual use versus cigarettes, *NEJM Evid* 3 (2024) EVIDoa2300229.
- [11] S.H. Randell, R.C. Boucher, University of North Carolina Virtual Lung G: effective mucus clearance is essential for respiratory health, *Am. J. Respir. Cell Mol. Biol.* 35 (2006) 20–28.
- [12] G. Singh, S.L. Katal, Clara cell proteins, *Ann. N. Y. Acad. Sci.* 923 (2000) 43–58.
- [13] E.L. Rawlins, T. Okubo, Y. Xue, D.M. Brass, R.L. Auten, H. Hasegawa, F. Wang, B.L. Hogan, The role of Scgb1a1+ Clara cells in the long-term maintenance and repair of lung airway, but not alveolar, epithelium, *Cell Stem Cell* 4 (2009) 525–534.
- [14] L. Miyashita, G. Foley, E-cigarettes and respiratory health: the latest evidence, *J. Physiol.* 598 (2020) 5027–5038.
- [15] M. Tsai, M.K. Byun, J. Shin, Alexander LE. Crotty, Effects of e-cigarettes and vaping devices on cardiac and pulmonary physiology, *J. Physiol.* 598 (2020) 5039–5062.
- [16] J.L. Carson, L. Zhou, L. Brighton, K.H. Mills, H. Zhou, I. Jaspers, M. Hazucha, Temporal structure/function variation in cultured differentiated human nasal epithelium associated with acute single exposure to tobacco smoke or E-cigarette vapor, *Inhal. Toxicol.* 29 (2017) 137–144.
- [17] C.S. Tellez, M.J. Grimes, D.E. Juri, K. Do, R. Willink, W.W. Dye, G. Wu, M.A. Picchi, S.A. Belinsky, Flavored E-cigarette product aerosols induce transformation of human bronchial epithelial cells, *Lung Cancer* 179 (2023) 107180.
- [18] G.E. Duclos, V.H. Teixeira, P. Autissier, Y.B. Gesthalter, M.A. Reinders-Luinge, R. Terrano, Y.M. Dumas, G. Liu, S.A. Mazzilli, C.A. Brandsma, et al., Characterizing smoking-induced transcriptional heterogeneity in the human bronchial epithelium at single-cell resolution, *Sci. Adv.* 5 (2019) eaaw3413.
- [19] D. Jiang, N. Schaefer, H.W. Chu, Air-liquid interface culture of human and mouse airway epithelial cells, *Methods Mol. Biol.* 1809 (2018) 91–109.
- [20] C.H.T. Bui, R.W.Y. Chan, M.M.T. Ng, M.C. Cheung, K.C. Ng, M.P.K. Chan, L.L.Y. Chan, J.H.M. Fong, J.M. Nicholls, J.S.M. Peiris, M.C.W. Chan, Tropism of influenza B viruses in human respiratory tract explants and airway organoids, *Eur. Respir. J.* 54 (2019).
- [21] C. Leung, S.J. Wadsworth, S.J. Yang, D.R. Dorscheid, Structural and functional variations in human bronchial epithelial cells cultured in air-liquid interface using different growth media, *Am. J. Physiol. Lung Cell Mol. Physiol.* 318 (2020) L1063–L1073.
- [22] H.H. Bragulla, D.G. Homberger, Structure and functions of keratin proteins in simple, stratified, keratinized and cornified epithelia, *J. Anat.* 214 (2009) 516–559.
- [23] F. Kuonen, N.Y. Li, D. Haensel, T. Patel, S. Gaddam, L. Yerly, K. Rieger, S. Aasi, A.E. Oro, c-FOS drives reversible basal to squamous cell carcinoma transition, *Cell Rep.* 37 (2021) 109774.
- [24] S. Kalkhoran, S.A. Glantz, E-cigarettes and smoking cessation in real-world and clinical settings: a systematic review and meta-analysis, *Lancet Respir. Med.* 4 (2016) 116–128.
- [25] C. Glynos, S.I. Bibli, P. Katsaounou, A. Pavlidou, C. Magkou, V. Karavana, S. Topouzis, I. Kalomenidis, S. Zakyntinos, A. Papapetropoulos, Comparison of the effects of e-cigarette vapor with cigarette smoke on lung function and inflammation in mice, *Am. J. Physiol. Lung Cell Mol. Physiol.* 315 (2018) L662–L672.
- [26] M. Chaumont, P. van de Borne, A. Bernard, A. Van Muylem, G. Deprez, J. Ullmo, E. Starczewska, R. Briki, Q. de Hemptinne, W. Zaher, N. Debbas, Fourth generation e-cigarette vaping induces transient lung inflammation and gas exchange disturbances: results from two randomized clinical trials, *Am. J. Physiol. Lung Cell Mol. Physiol.* 316 (2019) L705–L719.
- [27] H.R. Park, M. O'Sullivan, J. Vallarino, M. Shumyatcher, B.E. Himes, J.A. Park, D.C. Christiani, J. Allen, Q. Lu, Transcriptomic response of primary human airway epithelial cells to flavoring chemicals in electronic cigarettes, *Sci. Rep.* 9 (2019) 1400.
- [28] G.L. Pozuelos, M. Kagda, M.A. Rubin, M.L. Goniewicz, T. Girke, P. Talbot, Transcriptomic evidence that switching from tobacco to electronic cigarettes does not reverse damage to the respiratory epithelium, *Toxics* 10 (2022).
- [29] M.A. Song, S.A. Reisinger, J.L. Freudenheim, T.M. Brasky, E.A. Mathe, J.P. McElroy, Q.A. Nickerson, D.Y. Weng, M.D. Wewers, P.G. Shields, Effects of electronic cigarette constituents on the human lung: a pilot clinical trial, *Cancer Prev. Res.* 13 (2020) 145–152.
- [30] M. Tsai, M.A. Song, C. McAndrew, T.M. Brasky, J.L. Freudenheim, E. Mathe, J. McElroy, S.A. Reisinger, P.G. Shields, M.D. Wewers, Electronic versus combustible cigarette effects on inflammation component release into human lung, *Am. J. Respir. Crit. Care Med.* 199 (2019) 922–925.
- [31] J.K. Watson, S. Rulands, A.C. Wilkinson, A. Wuidart, M. Ousset, A. Van Keymeulen, B. Gottgens, C. Blanpain, B.D. Simons, E.L. Rawlins, Clonal dynamics reveal two distinct populations of basal cells in slow-turnover airway epithelium, *Cell Rep.* 12 (2015) 90–101.
- [32] J.E. Boers, A.W. Ambergen, F.B. Thunnissen, Number and proliferation of clara cells in normal human airway epithelium, *Am. J. Respir. Crit. Care Med.* 159 (1999) 1585–1591.
- [33] M.Y. Cai, C.Y. Yip, K. Pan, Y. Zhang, R.W. Chan, W.Y. Chan, W.H. Ko, Role of carbon monoxide in oxidative stress-induced senescence in human bronchial epithelium, *Oxid. Med. Cell. Longev.* 2022 (2022) 5199572.
- [34] Y.J. Hou, K. Okuda, C.E. Edwards, D.R. Martinez, T. Asakura, K.H. Dinno 3rd, T. Kato, R.E. Lee, B.L. Yount, T.M. Mascenik, et al., SARS-CoV-2 reverse genetics reveals a variable infection gradient in the respiratory tract, *Cell* 182 (2020) 429–446 e414.
- [35] M.D. Johansen, R.M. Mahbub, S. Idrees, D.H. Nguyen, S. Miemczyk, P. Pathinayake, K. Nichol, N.G. Hansbro, L.J. Gearing, P.J. Hertzog, et al., Increased SARS-CoV-2 infection, protease, and inflammatory responses in chronic obstructive pulmonary disease primary bronchial epithelial cells defined with single-cell RNA sequencing, *Am. J. Respir. Crit. Care Med.* 206 (2022) 712–729.
- [36] C.T. Wohnhaas, J.A. Gindele, T. Kiechle, Y. Shen, G.G. Leparc, B. Stierstorfer, H. Stahl, F. Gantner, C. Viollet, J. Schymeinsky, P. Baum, Cigarette smoke specifically affects small airway epithelial cell populations and triggers the expansion of inflammatory and squamous differentiation associated basal cells, *Int. J. Mol. Sci.* 22 (2021).
- [37] A.M. Greaney, T.S. Adams, M.S. Brickman Raredon, E. Gubbins, J.C. Schupp, A.J. Engler, M. Ghaedi, Y. Yuan, N. Kaminski, L.E. Niklason, Platform effects on regeneration by pulmonary basal cells as evaluated by single-cell RNA sequencing, *Cell Rep.* 30 (2020) 4250–4265 e4256.
- [38] A.T. Reid, P.C. Veerati, R. Gosens, N.W. Bartlett, P.A. Wark, C.L. Grainge, S.M. Stick, A. Kicic, F. Moheimani, P.M. Hansbro, D.A. Knight, Persistent induction of goblet cell differentiation in the airways: therapeutic approaches, *Pharmacol. Ther.* 185 (2018) 155–169.
- [39] G. Chen, T.R. Korfhagen, C.L. Karp, S. Impey, Y. Xu, S.H. Randell, J. Kitzmiller, Y. Maeda, H.M. Haitchi, A. Sridharan, et al., Foxa3 induces goblet cell metaplasia and inhibits innate antiviral immunity, *Am. J. Respir. Crit. Care Med.* 189 (2014) 301–313.
- [40] J.M. Shin, M.S. Han, J.H. Park, S.H. Lee, T.H. Kim, S.H. Lee, The EphA1 and EphA2 signaling modulates the epithelial permeability in human sinonasal epithelial cells and the rhinovirus infection induces epithelial barrier dysfunction via EphA2 receptor signaling, *Int. J. Mol. Sci.* 24 (2023).
- [41] S.S. Jankauskas, D.W.L. Wong, R. Bucala, S. Djudjaj, P. Boor, Evolving complexity of MIF signaling, *Cell. Signal.* 57 (2019) 76–88.
- [42] P. Ekblom, P. Lonai, J.F. Talts, Expression and biological role of laminin-1, *Matrix Biol.* 22 (2003) 35–47.

- [43] Q. Wang, J.H. Lucas, C. Pang, R. Zhao, I. Rahman, Tobacco and Menthol flavored electronic cigarettes induced inflammation and dysregulated repair in lung fibroblast and epithelium, *Res. Sq.* 25 (1) (2023) 23.
- [44] S.M. Gaiha, J. Cheng, B. Halpern-Felsher, Association between youth smoking, electronic cigarette use, and COVID-19, *J. Adolesc. Health* 67 (2020) 519–523.
- [45] L. Martin-Sancho, M.K. Lewinski, L. Pache, C.A. Stoneham, X. Yin, M.E. Becker, D. Pratt, C. Churas, S.B. Rosenthal, S. Liu, et al., Functional landscape of SARS-CoV-2 cellular restriction, *Mol. Cell* 81 (2021) 2656–2668 e2658.
- [46] R. MacCann, A.A.G. Leon, G. Gonzalez, M.J. Carr, E.R. Feeney, O. Yousif, A.G. Cotter, E. de Barra, C. Sadlier, P. Doran, P.W. Mallon, Dysregulated early transcriptional signatures linked to mast cell and interferon responses are implicated in COVID-19 severity, *Front. Immunol.* 14 (2023) 1166574.
- [47] M. Manevski, S. Yogeswaran, I. Rahman, D. Devadoss, H.S. Chand, E-cigarette synthetic cooling agent WS-23 and nicotine aerosols differentially modulate airway epithelial cell responses, *Toxicol Rep* 9 (2022) 1823–1830.
- [48] S. Antherieu, A. Garat, N. Beauval, M. Soyey, D. Allorge, G. Garcon, J.M. Lo-Guidice, Comparison of cellular and transcriptomic effects between electronic cigarette vapor and cigarette smoke in human bronchial epithelial cells, *Toxicol. Vitro* 45 (2017) 417–425.
- [49] X. Mao, D. Zhou, K. Lin, B. Zhang, J. Gao, F. Ling, L. Zhu, S. Yu, P. Chen, C. Zhang, et al., Single-cell and spatial transcriptome analyses revealed cell heterogeneity and immune environment alternations in metastatic axillary lymph nodes in breast cancer, *Cancer Immunol. Immunother.* 72 (2023) 679–695.